THE AMERICAN SOCIETY OF MECHANICAL ENGINEERS
345 E. 47 St., New York, N.Y. 10017



90-GT-330

# Influence of High Rotational Speeds on the Heat Transfer and Discharge Coefficients in Labyrinth Seals

**W. WASCHKA, S. WITTIG, S. KIM**
Lehrstuhl und Institut für Thermische Strömungsmaschinen
Universität Karlsruhe (T.H.)
Kaiserstr.12, D-7500 Karlsruhe (West-Germany)

## ABSTRACT

Heat transfer and leakage loss measurements were obtained for compressible flows in typical straight-through labyrinth seals with high rotational speeds. The experiments are an extension of our earlier measurements in a stationary test facility. In order to ensure direct comparisons to the original experiments, the principal dimensions of the test facility and gas dynamic parameters of the hot gas were kept similar. The new study encompasses a wide range of Taylor numbers, Reynolds numbers and clearances between the rotating annular fins and the stationary shroud. Heat transfer coefficients are determined for the stator as well as for the rotor. Temperature measurements along the cooled rotor were performed utilizing a high accuracy telemetric system. Continuous clearance control was achieved by employing specially designed gauges. Detailed pressure and temperatur measurements in the axial as well as in the circumferential direction were performed. Heat transfer coefficients and loss parameters are presented and compared with those obtained under steady state conditions.

## NOMENCLATURE

A - Flow area, $m^2$
c - mass averaged axial velocity, m/s
d - Diameter of the fins, m
$C_D$ - Discharge coefficient
h - Fin height, m
$\dot{m}_{ideal}$ - ideal mass flow rate
n - Rotational speed, 1/min
p - Pressure, $N/m^2$
$\dot{Q}_{ideal}$ - Ideal flow function, $\sqrt{kg\ K/kJ}$
R - Specific gas constant, kJ/kg K
$r_w$ - Radius of the cavity, m
s - Gap width, m
t - Pitch, m
u - peripheral velocity of the cavity, m/s
$\alpha$ - heat transfer coefficient, $W/m^2$
$\mu$ - dynamic viscosity, kg/m s
$\rho$ - density, $kg/m^3$
$\kappa$ - isentropic coefficient

Subscripts:

crit - critical value
max - maximaum value
meas - measured value
o - settling chamber
$\infty$ - behind the seal

## INTRODUCTION

Despite advanced techniques such as gas-film seals, labyrinths remain the most important and widely used sealing elements in turbomachinery since their indroduction in steam turbines near the turn of the century. The main tasks of this contactless seal are to reduce the undesired leakage between the rotating and stationary components of the engine and to control the cooling air supply. A small clearance accomodates the differential thermal expansion between the rotating fins and the

*Presented at the Gas Turbine and Aeroengine Congress and Exposition—June 11-14, 1990—Brussels, Belgium
This paper has been accepted for publication in the Transactions of the ASME
Discussion of it will be accepted at ASME Headquarters until September 30, 1990

shroud as well as the centrifugal growth. Although this clearance allows parasitic losses it guarantees a high durability of the seal. As the resulting leakage strongly influences the performance level of the engine, many theoretical and experimental studies have been done to understand the fluid mechanics of labyrinths. The earlier analytic and experimental attempts by Martin, Stodola, Egli, Komotori and others are summerized in Trutnovsky's (1981) comprehensive book. Recent investigations are presented by Stocker (1978), Wittig (1982,87a,b,c), Dörr (1985), Jacobsen (1987), Schelling (1988). Wittig et al. and Schelling (1987a-c) perfomed numerical computations of the flow-field inside the labyrinth seal, using a finite-volume computer code based on the time-averaged turbulent Navier-Stokes equations and the k-e turbulence model. In verifying the experimental results, Wittig et al. (1987a-c) also solved the energy equation for the entire flow-field inside a straight-through and a stepped labyrinth seal. Utilizing the analogies between heat transfer and wall friction local heat transfer coefficients could be derived. The heat transfer from the hot gas to the labyrinth components is another important aspect for seal design, especially for the thermal expansions and -if utilized- for the active clearance control. But there are also detrimental effects of the heat transfer on the required air cooling system in a blade which is in contact with the seal and also on the durability of the seal itself, caused by the high temperature-gradients in the rotating fins. Heat transfer coefficients have been puplished only by a few authors, Sheinin (1961), Shvets (1963), Kapinos and Gura (1970,73), Kuznezow and Zuravlew (1972), Metzger and Bunker (1985), Wittig et al. (1987), Jacobsen (1987) and Schelling (1988).

However, most studies are based on the assumption that there is only a negligible effect of rotation on the leakage rate and heat transfer in labyrinth seals. Moreover, in most of the very few experiments including rotational effects, centrifugal growth and the thermal expansion was not measured and only in some cases theoretically considered. As the differential growth of rotor and stator often exceeds the cold stationary clearance, such a short-coming results in significant uncertainties in the calculated characteristic values. Therefore, it is not suprising that some of the puplished results are not in good agreement.

Becker (1907), apparently the first who considered this problem, found no rotational effects on the labyrinth flow. While Friedrich (1933) measured a 20 % leakage reduction in a straight-through labyrinth seal and Yamada (1962) observed a maximum increase of the drag coefficient by a factor 10, if the flow was laminar; but rotation had little impact on the seal flow, as soon as the flow became turbulent. The leakage increased by 13% in Morrison's and Chi's (1985) stepped seal but decreased by 9% in Stockers (1978) seal toward higher rotational speeds.

The majority of the studies, examining the effect of rotation on the seal flow, have been done numerically. Stoff (1980) predicted the incompressible flow in a straight-through labyrinth seal, but the computed domain was restricted to a single cavity. The resulting data and the corresponding LDA-measurements of mean swirl velocity in an enlarged water model differed by 7%. Demko et al. (1987) determined a second recirculating zone of the incompressible cavity flow at high rotational speeds. More details of the cavity flow were obtained by Demko et al. (1988) and Rhode et al. (1988,89). Their predictions are compared with hot-film measurements obtained in enlarged water models. The latest numerical and experimental work has been done by Wittig et al. (1989), examining rotational effects on the compressible flow as well as on heat transfer. Earlier heat transfer measurements were performed by the already mentioned authors, Sheinin, Shvets, Dyban, Khavin, Kapinos and Gura, but no significant effects of rotation were found. Recent studies by McGreehan (1989) indicate a significant windage power dissipation for high speeds, which reduces the leakage mass due to the Raleigh line effect but augments the thermal load of the seal material.

Further, it is well known, that in the absence of a dominant axial flow, rotation drastically augments the heat transfer (i.e. Patankar and Murthy, 1982) between the hot gas and the cooled labyrinth components.

Of course, the basic assumption, that rotation has little impact on the seal flow is valid for many conditions, tested by numerous authors. However, despite, the considerable quantitative differences in the measured rotational effects on the labyrinth flow and heat transfer, the studies also have demonstrated that rotation can not be neglected at small axial Reynolds numbers and high Taylor numbers. While, in the past, there were few relevant applications, recent advances in seal design produce high pressure labyrinth seals which operate at high speed and low leakage rates. Furthermore, the shaft speed in modern turbomachinery becomes very high and the peripheral velocity of the tip of the fin reaches supersonic velocities in some cases. Active clearance control and special abradable coatings on the non-rotating stator allow tighter clearances and lead to lower leakage-rates and higher ratios of axial to peripheral velocity. These developments require more accurate predictions for the design of modern engines, taking into account the geometry of the entire labyrinth. To verify numerical results and to improve available Navier-Stokes finite volume computer codes, detailed measurements under realistic conditions are required. This includes information about the onset of rotational effects, in regard to leakage rate and heat transfer.

Although, as a consequence of the wide application a lot of different seal-geometries are developed, gasdynamic effects can be studied on basic configurations as:

- Annular gap
- Straight-through labyrinth
- Stepped labyrinth
- "Real" or staggered labyrinth

The annular gap and the straight-through labyrinth seals were the first geometries studied in the present research, stepped and staggered labyrinths will follow.

## EXPERIMENTAL FACILITY AND INSTRUMENTATION

Our previously described test-facility (Wittig et al.,1987a,b,c), where plane configurations have been studied, was extended by a new test section for high rotating labyrinth seals. The test facility is shown schematically in Figure 1. Air is supplied by compressors with a pressure ratio of 4.0 and a maximum mass flow of 0.5 kg/s. The compressed air is recooled by an intercooler. The supply pressure is kept constant at 3.5 bar by means of a bypass valve, which guarantees uniform conditions for mass flow measurements. The mass flow rate is determined by one of three orifice meters, applicable to the appropriate measurement range and connected to a precision water pressure gauge. The electrical heater is designed for a maximum exit temperature of 400 C and can be controlled continuously from 0-150 kW. A specially designed settling chamber is used to obtain velocity and temperature profiles before entering the new test section which is shown in Figure 2. The thick-walled housing (position 5) of the test section is mounted directly behind the settling chamber. The flow exits via a large Carnot diffusor, which provides constant pressure conditions at the exit of the seal. The labyrinth seal in the test section consists of an inner rotating part (pos.2) with six fins (diameter: 250 mm, pitch: 12 mm, thickness of the fins: 2.5 mm ) and a stationary

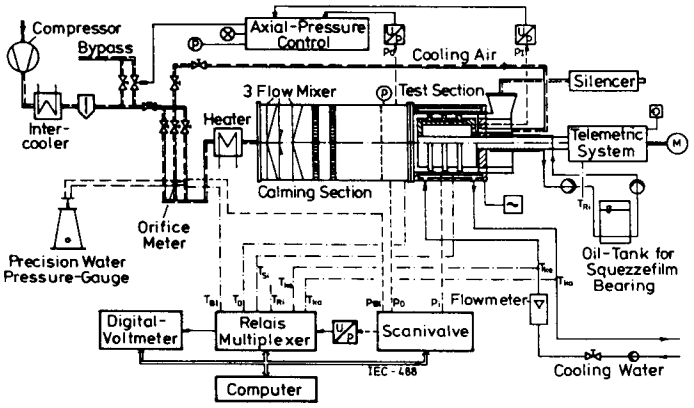


Fig. 1 Labyrinth seal test facility

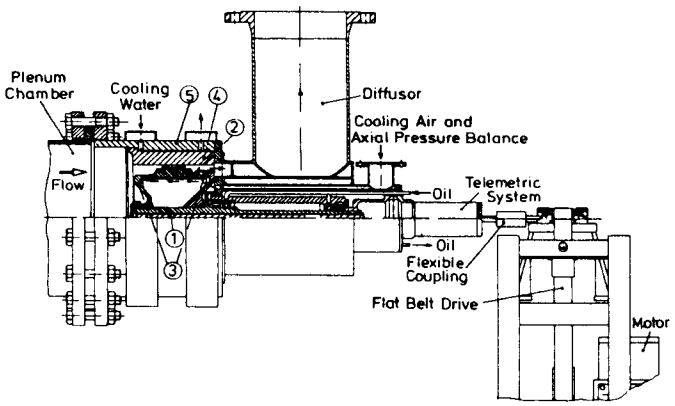


Fig. 2 Test section for rotating labyrinth seals

outer smooth part (pos. 4), the stator. Due to experimental requirements a scaled-up model (5:1) was used. Three stators with different inner diameters (251, 252 and 252.6 mm) were biult to study clearance effects. The rotor consists of the shaft (pos.1) , the earlier mentioned inner part of the seal (pos. 2) and the seal-supporters (pos. 3), Press-fittings are used to avoid small local displacements of the components after mounting. Also, a special rotor design was required to ensure a constant clearance distribution in axial and azimuthal directions, during the diameter growth due to the centrifugal forces.

A "flying" rotor-support (both bearings are on the right hand side of the seal) was chosen to provide undisturbed flow conditions at the entrance of the seal. The support also allows good exchangeability of the stators and there is no need for an extensive bearing cooling system, as both bearings are in the cold region of the test section. High precision spindle bearings with an extremely small bearing play reduce rotor eccentricity and displacement to a minimum. Rotordynamic vibrations are kept small, using an additional damping squeeze-film between the outer bearing box and the housing. (Film-thickness: 80 $\mu m$, damping coefficient: 2 Ns/mm). This configuration provides for (overcritical) operating conditions above the first Eigenfrequency of the rotor. The rotor rotates therefore at all speeds

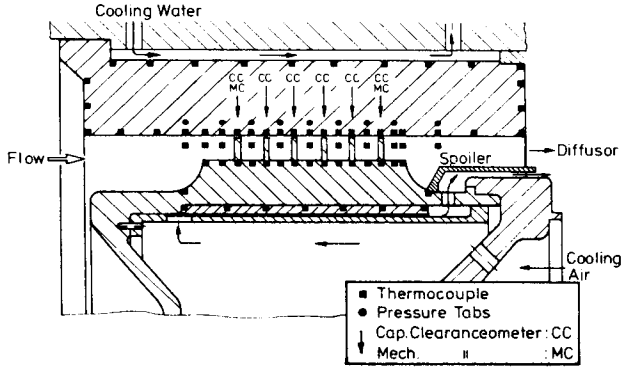


Fig. 3 Schematic instrumentation in one cross-sectional area

around its mass-centerline dislocated by the mass-eccentricity to the centerline of the bearings. A precise balancing under operating conditions reduces the eccentricity to approximately 5 $\mu m$. However, it should be mentioned that the squeeze-film were built up only for speeds below the first critical speed ( 2500 rpm) while the outer bearing box is sitting on the housing. As a consequence, all measurements in this range of speed were done only with conventional bearing. To reduce the high axial pressure thrust on the bearings the air cooling system of the rotor, used for heat transfer measurements, was combined with a thrust balance. Therefore, the cooling air is lead through channels in the housing to a chamber downstream of the rotor. Based on the measured pressures in the two opposing chambers and the relevant rotor regions the rest load is calculated to adjust the pressure of the cooling air. Furthermore, the air flows into the rotor-chamber and through the annular gap along the inner side of the rotating seal to the diffusor behind the seal. A spoiler is used to separate the cooling air and the leakage flow directly behind the seal. This combination of cooling air system and thrust balance includes the desired effect, that the cooling mass flow rate depends on the pressure in the settling chamber and so indirectly on the leakage mass flow through the seal. The amount of the cooling rate is automatically adjusted to the level of heat transfer from the hot gas to the seal. Also, regarding the Biot-number, wall thickness and thermal conductivity were adapted at the expected heat-transfer coefficient to have a maximum of accuracy for the finite-element method used.

Water was used as the cooling fluid for the heat-transfer measurements on the stator. The annular gap for the water cooling is separated in several axial chambers. The water flow can be controlled by valves located at the exit of each chamber.

## Instrumentation

Surface temperatures of the stator and the rotor and the gas temperatures were measured by NiCr-Ni (Type J) thermocouples (diameter 0.5 mm). The stator was instrumented in three different cross-sections, to provide information for the required water cooling and also about probable rotor-dynamic effects on heat-transfer. The gas temperatures were also recorded at three different cross-sections in the plenum chamber, in the center of each cavity and at the exit of the seal. The 27 thermocouples of the rotor are an intergral to the rotating part of the telemetrical system, which includes, time-multiplexer, amplifier, temperature-compensation and frequency-modulation of the signals. The modulated signals and a reference signal are sent to the stationary part of telemetrical system demodulated and again separated. The uncertainty of the calibrated system is less than 1 K. The pressure distribution inside the seal was obtained in three different cross-sections from pressure taps in the stator. All values , including the settling chamber pressure and the pressure behind the labyrinth seal are determined by an absolute pressure-gauge in connection with a scannivalve. A precision water pressure-gauge was used in the case of small pressure differences over the seal. The principle instrumentation is shown in Figure 3.

## Clearance measurements

A positive clearance measurement is one of the most critical elements for an accurate analysis and description of the measured heat transfer and the leakage losses, because centrifugal growth and thermal expansions reach at some cases 50% of the original clearance. Therefore, an extensive amount of work was done for exact clearance measurements. A total number of ten capacitive clearanceometers and six mechanical gauges are mounted in the stator above the fins of the rotor. Three mechanical and three capacitive clearanceometers are mounted above the first and the last fin, to compute in addition the eccentricity of the rotor. Above each of the other fins one further capacitive clearanceometer is available. The small fins ( 2.5 mm) and the relatively great gap ( 0.5, 1.0 and 1.3 mm) required a special, small designed sensitive area (0.8 mm · 30 mm) of the clearanceometers. The operating temperature is limited by the isolation material to 250 C. The measurement frequency is 17 kHz. The mechanical gauges are used only for control puposes. In Figure 4 the entire fin-averaged gap width is presented as a function of the rotational speed for a cold gas and hot gas, for the pressure ratio 1.26 . All pressure, temperature and capacitive signals as well as the rotational speed are recorded by a data acquisition system and processed.

The rotor is driven by an electrical motor (max. 3000 rpm) in connection with a flat belt drive (ratio 1:7). An extremly flexible coupling is located between the belt drive and the rotor.

The entire facility and the data acquisition was tested, utilizing an annular gap geometry. The calculated discharge coefficients and heat transfer coefficients of the annular gab have been compared with literature values and excellent agreement obtained.

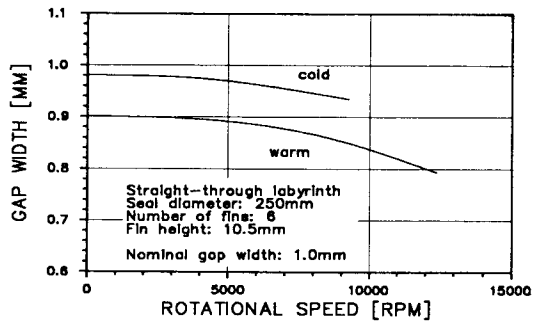


Fig. 4 The influence of rotational speed on the gap width

## EXPERIMENTAL RESULTS AND DISCUSSION

For direct comparisons with our earlier measurements in a stationary test facility (Wittig et al., 1987), the same dimensionless mass flow parameter was used, to describe and analyse the labyrinth seal losses. The flow discharge coefficient is defined as:

$$C_D = \frac{\dot{m}_{meas}}{\dot{m}_{ideal}} \tag{1}$$

where $m_{ideal}$ is determined as the mass flow through an ideal nozzle, with the same cross-sectional flow area as in the gap of the labyrinth seal and same entire pressure ratio. $m_{ideal}$ is calculated in the usual way

$$\dot{m}_{ideal} = \frac{\dot{Q}_{ideal} \cdot p_o \cdot A}{\sqrt{T_o}} \tag{2}$$

with

$$\dot{Q}_{ideal} = \left(\frac{p_\infty}{p_o}\right)^{\frac{1}{\kappa}} \sqrt{\frac{2\kappa}{R \cdot (\kappa - 1)} \left[1 - \left(\frac{p_\infty}{p_o}\right)^{\frac{\kappa-1}{\kappa}}\right]} \tag{3}$$

for subcritical pressure ratios. For supercritical pressure ratios the value of $Q_{ideal}$ is equal to the maximum value at

$$\left(\frac{p_\infty}{p_o}\right)_{crit} = \left(\frac{2}{\kappa + 1}\right)^{\frac{\kappa}{\kappa-1}} \tag{4}$$

The actual, speed-dependent cross-sectional area is determined by averaging the continuously measured clearances as described.

The local heat transfer coefficient is derived from

$$\alpha = \frac{d\dot{Q}}{dA \cdot (T_G - T_W)} \tag{5}$$

with

$$d\dot{Q} = -\lambda \cdot \nabla \cdot T_{|wall} \tag{6}$$

The local heat flux dQ is determined from the two dimensional temperature distribution in the stator and the rotor. The temperature distribution is caculated from the wall temperatures, utilizing a finite-element program. The wall temperatures $T_W$ at each boundary knot of the finite-element net are interpolated from local measured values by rational spline functions. The gas temperature $T_G$ was also determined from local measurements. For the fin region, the calculated heat transfer coefficient is equivalent with a fin heat transfer coefficient, as the only fin temperatur ($T_W = T_{Wr}$ ) was measured in the fin root. In addition, mean heat transfer coeffients were caculated by averaging the local values. The averaged coefficients for the stator refer to the total flow exposed surface, whereas the averaged coefficients for the rotor describe the total heat flux normalized to the rotor surface without fins. The reference gas and wall temperatures have been averaged from the local values.

The rotational effect is described by the ratio of the Taylor number to the axial Reynolds number. These dimensionless

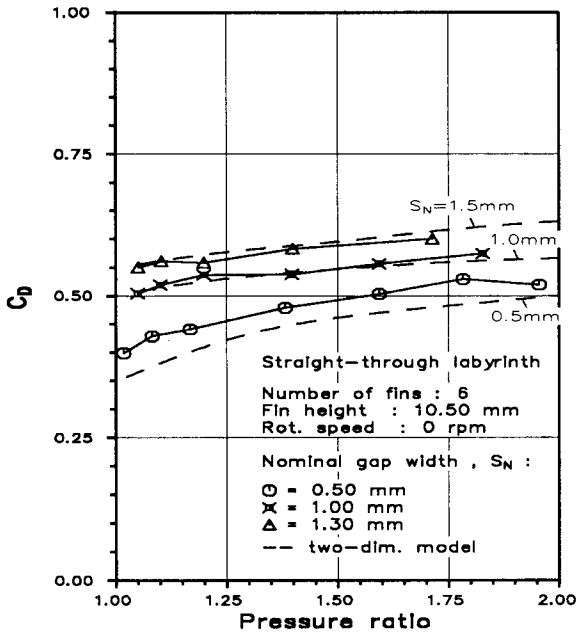


Fig. 5 Discharge coefficients without rotation, comparisation with the two-dimensional models

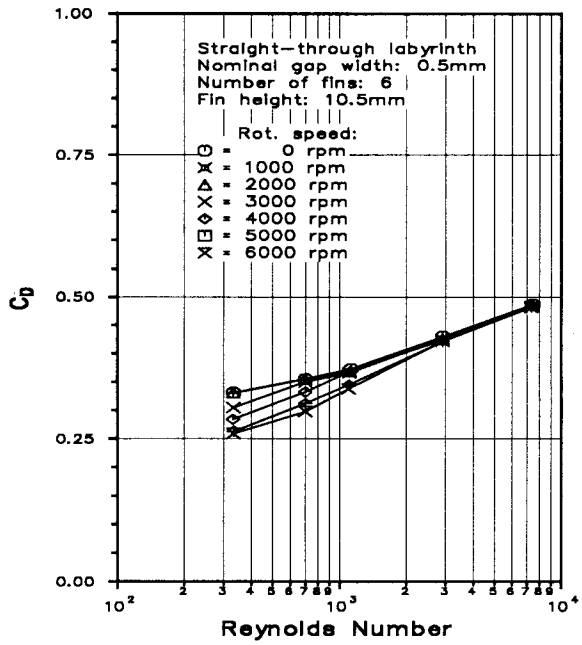


Fig. 6 Rotational effects as a function of the Reynolds number ( $s_N = 0.5mm$)

numbers are defined as

$$Ta = \frac{u_w \cdot 2 \cdot s}{\nu}\sqrt{\frac{s}{r_w}} \qquad Re = \frac{\dot{m}_{meas}}{\bar{\mu} \cdot \pi \cdot r_w} \tag{7}$$

This combination can be regarded as the ratio of axial to peripheral momentum. However, it should be kept in mind, that the application of the Taylor number as a criterion for stable operations is only valid for flows between rotating cylinders. While the well known Taylor vortices in annular gaps are caused by hydrodynamic instabilities, the origin of a second recirculation zone in the labyrinth cavity is due to the boundary conditions at the rotating fins. As a consequence, it can be expected that the rotational effects are strongly dependent on the labyrinth seal geometry, especially the cavity design.

For the experimental procedere discussed, the rotational speed was varied for each pressure ratios selected. In order to achieve comparability with our earlier experiments in flat models (scale 5:1), Figure 5 presents the experimentally derived discharge coefficients without rotation as a function of the pressure ratio and the gap width. Considering side wall effects in the flat model, the agreement is excellent. The pressure distribution, geometry variations and scaling effects are discussed elsewhere by Wittig et al. (1982, 87a,b,s).

Figures 6,7 and 8 show the influence of rotational speeds on the discharge coefficients as a function of the Reynolds number. A large decrease of the discharge coefficients toward higher rotational speeds is evident at low Reynolds numbers. At the smallest Reynolds number (Re=2000) and highest speed (10 000 rpm) a 25 % reduction of the discharge coefficient was obtained. The comparision between Figures 6,7 and 8 reveals an upper limit of the rotational effects at Reynolds numbers approximately of 5000 to 10 000, dependent of the clearance. The limiting Reynolds number seems to increase with increasing clearance. This behaviour agrees with the results of Yamada (1962), who measured a strong dependence of the resistance coefficient from the ratio $\frac{s}{r_w}$ . Another interesting observation, regarding the limiting Reynolds numbers, is that these values coincide fairly well with our earlier measurements with the stationary test facility, indicating a transition along the smooth stator wall from laminar to turbulent flow at Reynolds numbers approximately of 6000. This also confirms the results of Yamada for a flow between rotating coaxial cylinders with rectangular grooves, as far as his results show a dramatic increase of the resistance coefficient with increasing rotational speeds, when the flow was laminar, but only a negligible effect if the flow was already turbulent. It seems that, although in purely laminar flows, axial and peripherial flow-components are first independent of each other leading only to an increase of the shaft-torque, beyond a certain critical peripheral speed a

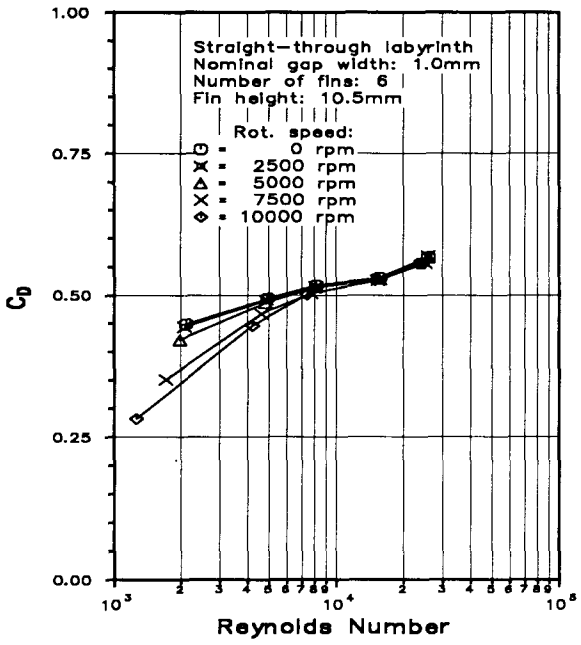


Fig. 7 Rotational effects as a function of the Reynolds number ( $s_N = 1.0mm$)

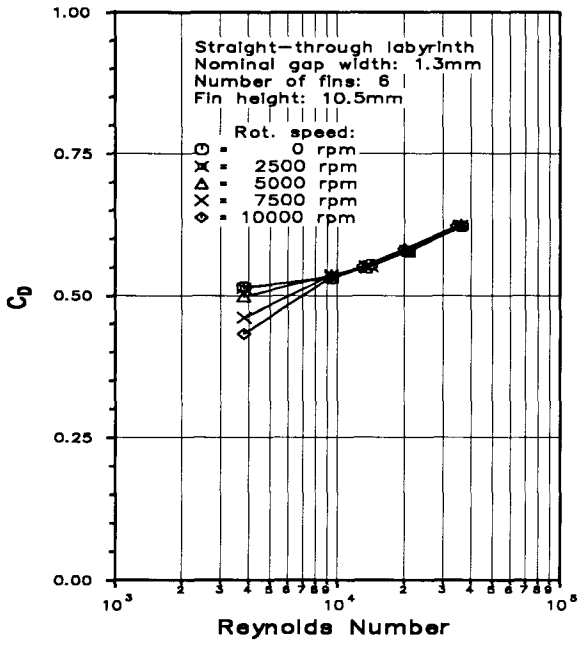


Fig. 8 Rotational effects as a function of the Reynolds number ( $s_N = 1.3mm$)

second vortex originates, which augments drastically the flow resistance. Although, in turbulent flows, axial and peripheral flow-components are no longer independent and there is a continuous increase of turbulence with higher rotational speeds, it should be noted that a high azimuthal velocity is required,

indicated by the peripheral to axial momentum, to obtain a domination of the swirl. Otherwise, the dividing stream line between the main stream and the cavity flow is shifted more and more outward due to the increasing centrifugal forces as shown by Demko et al.(1987), thus increasing the carry-over effect, as the stagnation point at the downstream cavity wall also shifts outward. However, if a second vortex is established at very high shaft speeds, an increase of flow-resistance can be expected. This however is not in relevence in most technical applications. Figures 9, 10 and 11 indicate the influence of the momentum ratio, including the geometry-factor $\frac{s}{r_w}$ for general physically similarity, on the discharge coefficients. A comparision between these figures reveals a critical ratio $\mathrm{Ta/Re}_{crit}$ of approximately 0.2 for all clearances. Demko et al. (1987) computed a critical value of 0.9 for the incipience of a second vortex. Demko's prediction was based on measured inlet boundary conditions of a cavity. Although the ratio $\frac{s}{r_w} = \frac{0.178mm}{38.6mm}$ of Demko's seal is similar to our ratio $\frac{s}{r_w} = \frac{0.5mm}{114.5mm}$ , Demko's cavity is 75 % tighter, which increases the resistance against an origination of a second recirculation flow. A final clarification of this problem is expected from our momentary numerically investigations, regarding rotational effects on the flow and the heat transfer in the same labyrinth geometries as used for the experimental part of our studies.

The influence of rotation on heat transfer is presented in Figure 12, for the nominal clearance $s_N = 1.0$ mm. In Figure 12a, the determined global Nusselt numbers for the rotor and the stator, without rotation, are compared with our earlier measurements in a flat model. The data obtained from the three dimensional model agree very well with that obtained from the two dimensional model. The relative increase of the Nusselt number, based on the Nusselt number achieved at no rotation,

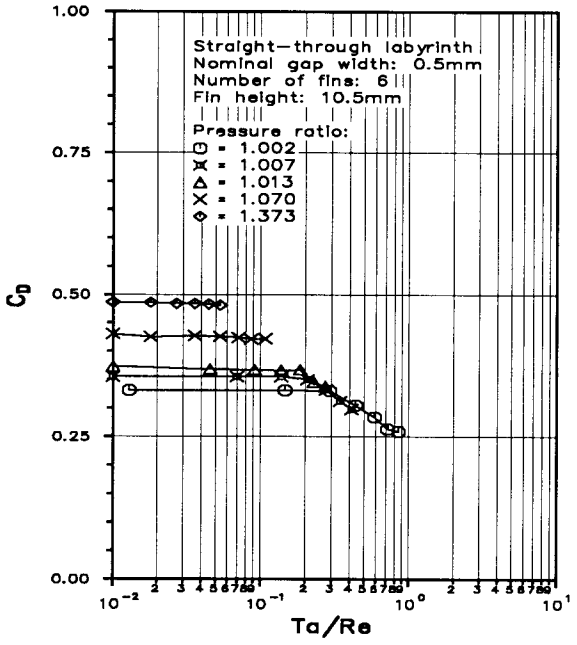


Fig. 9 Rotational effects on the discharge coefficients as a function of the ratio Ta/Re. ( $s_N = 0.5mm$)

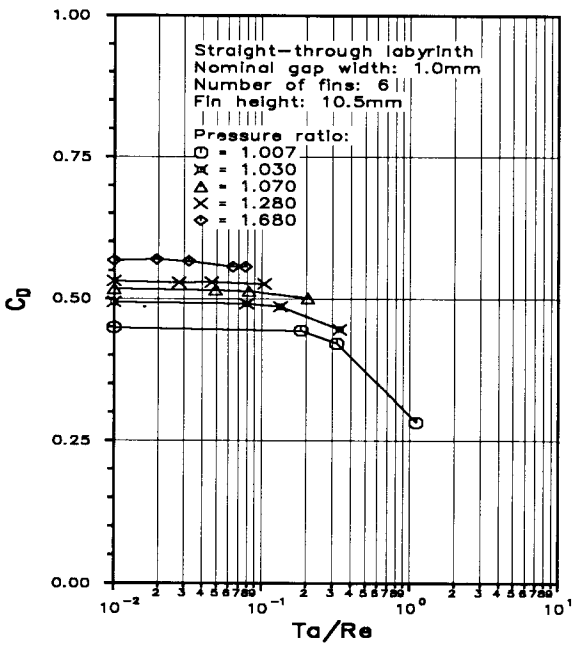


Fig.10 Rotational effects on the discharge coefficients as a function of the ratio Ta/Re. ( $s_N = 1.0mm$)

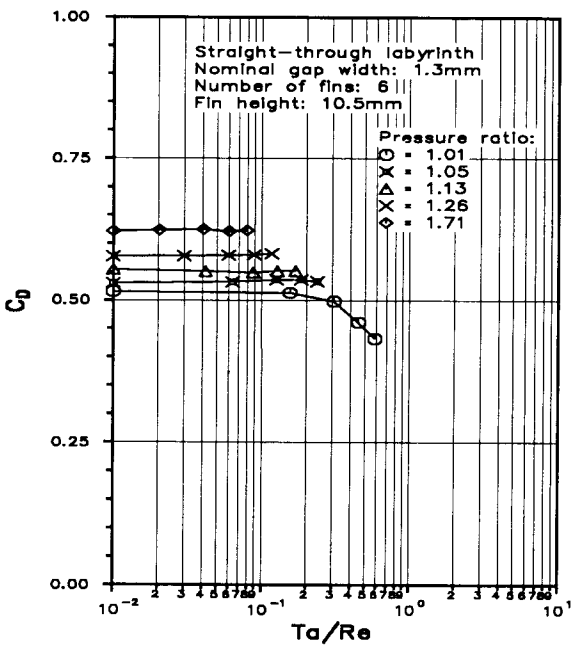


Fig.11 Rotational effects on the discharge coefficients as a function of the ratio Ta/Re. ( $s_N = 1.3mm$)

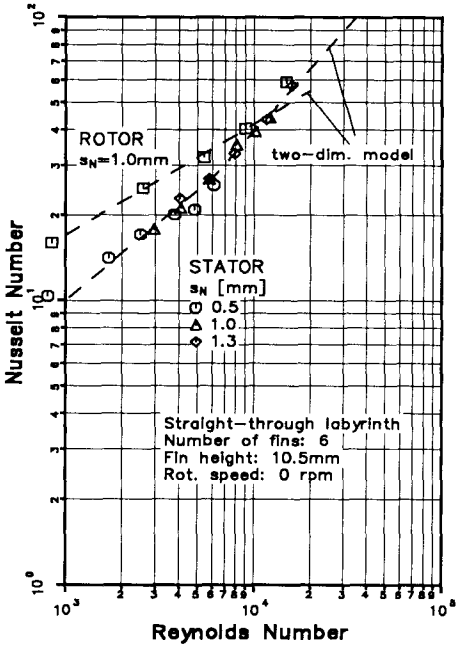


Fig.12a Global Nusselt numbers, comparison with the results of the two-dimensional models.

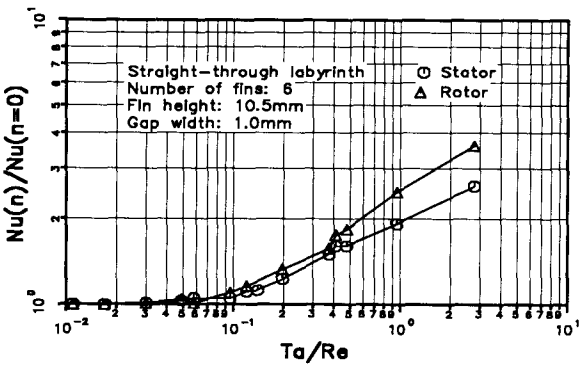


Fig.12b Rotational effects on the global Nusselt numbers as a function of the ratio Ta/Re. ( $s_N = 1.0mm$)

is shown in Figure 12b as a function of the ratio Ta/Re. The increase of the Nusselt number starts approximately at a ratio Ta/Re = 0.1 and reaches a factor of three at the maximum speed and the smallest Reynolds number. The rotational effects are slightly higher on the rotor than on the stator. The distributions of the local heat transfer coefficients on the labyrinth surface of the rotor and the stator are plotted in Figures 13 and 14, respectively for a pressure ratio of 1.26. It should be noted that the computed values at the fin root of the rotor (Fig. 13) are fin heat transfer coefficients as described earlier. Thus they are a good indication for rotational effects on the local heat flux and also on the global heat transfer. The local heat flux is highest at the root of the fins.

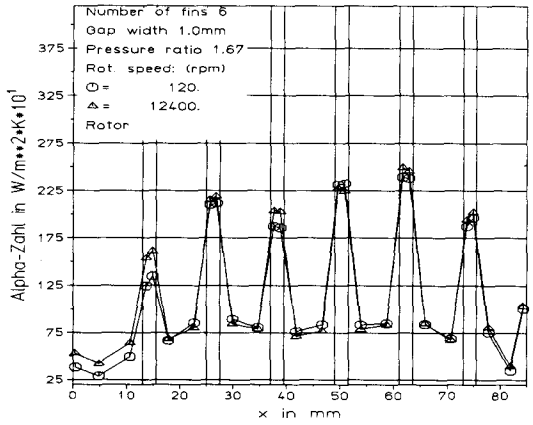


Fig.13 Local heat transfer coefficients for the rotor. ( $s_N = 1.0mm$)

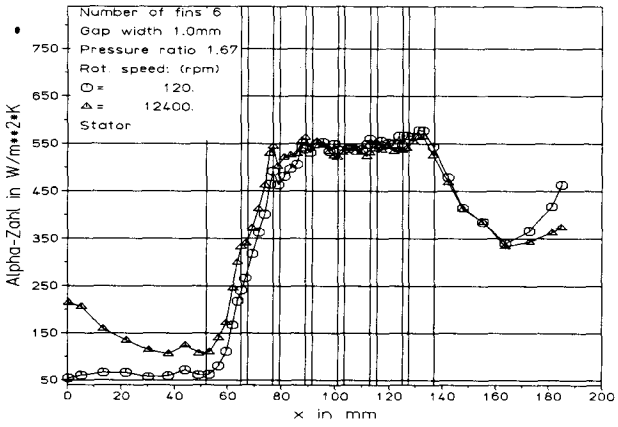


Fig.14 Local heat transfer coefficients for the stator. ( $s_N = 1.0mm$)

At the stator, the highest rise of the heat transfer is observed upstream of the labyrinth entrance. Here the axial velocty is relatively small and thus, the heat transfer is dominated by the preswirl. Due to the high accelaration of the flow at the entrance of the first fin, the influence of the swirl decreases drastically. The heat transfer distribution indicates a maximum above the fins and an increase of 12,400 rpm of about 10 %, compared to the nonrotating case.

## SUMMARY

A new test facility was presented, where heat transfer and leakage rate measurements for compressible flows in a straight-through labyrinth seal with high rotational speeds have been performed. Heat transfer coefficients have been experimentally determined for the stator as well as for the rotor , utilizing a high accuracy telemetric system. Specially designed capaci-

tive clearance gauges guarantee a detailed continuous clearance measurement.

Heat transfer and discharge coefficients under steady state conditions agree very well with earlier measurements in a two-dimensional model. The results show a significant effect of the rotation beyond a ratio Ta/Re approximately of 0.2, which reduces the leakage rate and increases the heat transfer. Future work is directed towards experimental and numerical investigations of stepped and staggered labyrinth seals.

## LITERATURE


Becker, E. (1907): Strömungsvorgänge in ringförmigen Spalten und ihre Beziehung zum Poiseuilleschen Gesetz. VDI-Forschungsheft 48, Berlin: VDI-Verlag, 1907, p.1-42.

Chi ,D.; G. L. Morrison (1985): Incompressible Flow in Stepped Labyrinth Seals. ASME 85-FE-4.

Demko, J. A.; G. L. Morrison; D. L. Rhode (1987): Effect of Shaft Rotation on the Incompressible Flow in a Labyrinth Seal. Proc. of the 5th International Conference on Numerical Methods in Laminar and Turbulent Flow, Canada.

Demko, J. A.; G. L. Morrison; D. L. Rhode (1988): Prediction and Measurement of Incompressible Flow in a Labyrinth Seal.AIAA-88-0190, 26th Aerospace Sciences Meeting

Dörr, L. (1985): Modellmessungen und Berechnungen zum Durchflussverhalten von Durchblicklabyrinthen unter Berücksichtigung der Übertragbarkeit. Dissertation, Institut für Thermische Strömungsmaschinen der Universität Karlsruhe .

Friedrich, H. (1933): Untersuchungen über das Verhalten der Schaufelspaltdichtungen in Gegenlauf-Dampfturbinen. Dissertation, Institut für Thermische Strömungsmaschinen der Universität Karlsruhe .

Jacobsen, K (1987): Experimentelle Untersuchungen zum Durchfluß und Wärmeübergang in Durchblick- und Stufenlabyrinthdichtungen Dissertation, Institut für Thermische Strömungsmaschinen der Universität Karlsruhe .

Kapinos, V. M.; L. A. Gura (1970): Investigation of Heat Transfer in Labyrinth Glands on Static Models. Thermal Engineering, Vol.17, Nr.11, p.53-56.

Kapinos, V.M.; L.A. Gura (1973): Heat Transfer in a Stepped Labyrinth Seal. Teploenergetika, 20 (6), p.22-25.

Kuznezov, A.L.; O.A. Zuravlov (1972): Wärmeübergang in den Labyrinthdichtungen von Gasturbinen (russisch). Energomashinostroenie, Nr.5, p.10-12.

Mcgreehan, W. F.; Ko, S. H. (1989): Power Dissipation in Smooth and Honeycomb Labyrinth Seals ASME-Papers, 89-GT-220.

Metzger, D.E.; R.S. Bunker (1985): Heat Transfer for Flow through Simulated Labyrinth Seals. Symposium on Transport Phenomena in Rotating Machinery, USA.

Patankar, S.V. and J.Y. Murthy (1982): Analysis of Heat Transfer from a Rotating Cylinder with Circumferential Fins. Symposium on Heat and Mass Transfer in Rotating Machinery, Dubrovnik, Yugoslavia.

Rhode, D. L.; S. H. Demko and G. L. Morrison (1988): Numerival and Experimental Evaluation of a new Low-Leakage Labyrinth Seal AIAA/ASME 88-2884, 24th Joint Propulsion Conference, Boston

Rhode, D. L.; R. I. Hibbs (1986): A Comparative Investigation of Corresponding Annular and Labyrinth Seal Flowfields. ASME-Papers, 89-GT-195.

Schelling, U. (1988): Numerische Berechnung kompressibler Strömungen mit Wärmeübergang in Labyrinthdichtungen. Dissertation, Institut für Thermische Strömungsmaschinen der Universität Karlsruhe .

Sheinin, E.I. (1961): Experimentelle Untersuchung des Wärmeübergangs in der Zone der Endabdichtung der Gasturbinen (russisch). Energomashinostroenie, Nr.1, p.25-27.

Shvets, I. T.; V. Y. Khavin; E. P. Dyban (1963): Heat Exchange in Labyrinth Seals of Turbine Rotor (russ). Energomashinostroenie, Vol.12, p.8-12.

Stocker, H.L. (1978): Determining and Improving Labyrinth Seal performance in Current and Advanced High Performance Gas Turbines. AGARD-CP-237.

Stoff, H. (1980): Incompressible Flow in a Labyrinth Seal. Journal of Fluid Mechanics, Vol.100, Part 4, p.817-829.

Trutnovsky, K. (1981): Berührungsfreie Dichtungen. VDI-Verlag, Düsseldorf, 1981.

Wittig, S. L. K.; L. Dörr; S. Kim (1982): Scaling Effects on Leakage Losses in Labyrinth Seals. Journal of Engineering for Power, Transactions of the ASME 82-GT-157.

Wittig, S. L. K.; K. Jacobsen; U. Schelling; S. Kim (1987): Experimentelle und theoretische Untersuchungen zum Durchflußverhalten und Wärmeübergang in Labyrinthen. Abschlußbericht FVV, Vorhaben Nr.293, 343, Heft 391.

Wittig, S. L. K.; K. Jacobsen; U. Schelling; S. Kim (1987): Heat Transfer in Stepped Labyrinth Seals. ASME , 87-GT-92.

Wittig, S. L. K.; U. Schelling; S. Kim; K. Jacobsen (1987): Numerical Predictions and Measurements of Discharge Coefficients in Labyrinth Seals. ASME- Conference 87-GT-188, Anaheim, California 1987.

Wittig, S. L. K.; Waschka, W. and T. Scherer (1989): Einfluß der Rotation auf das Durchflußverhalten und den Wärmeübergang in Labyrinthdichtungen. FVV-Informationstagung, Bad Orb, 1989

Yamada, Y. (1962): On the Pressure Loss of Flow between Rotating Co-Axial Cylinders with Rectangular Grooves. Bull. of ISME 5, Nr.20, p.642-651.